

## Photoluminescence studies of SnO<sub>2</sub> nanoparticles synthesized by chemical co-precipitation method: Effect of pH

<sup>1</sup> Lakshmi Venkata Kumari P, <sup>2</sup> Harish GS, <sup>3</sup> Sreedhara Reddy P

<sup>1,3</sup> Department of Physics, Sri Venkateswara University, Tirupati, Andhra Pradesh, India

<sup>2</sup> Lecturer in Physics, Government Polytechnic, Satyavedu, Andhra Pradesh, India

### Abstract

SnO<sub>2</sub> nanoparticles were synthesized by using cost-effective chemical co-precipitation method. To study the influence of pH on structural and optical properties of SnO<sub>2</sub> nanoparticles, pH value was varied from 7-12. Structural, surface morphology, chemical analysis and luminescence properties of prepared SnO<sub>2</sub> nanoparticles were studied by X-ray diffraction (XRD), fourier transform infrared spectroscopy (FTIR), scanning electron microscope (SEM) attached with energy dispersive spectroscopy (EDS) and photoluminescence studies (PL). X-ray diffraction study reveals the nano-size particle distribution of the samples with tetragonal rutile structure in the range of 2 to 4 nm. FTIR spectra show the structural confirmation of SnO<sub>2</sub> nanoparticles. Various PL signals were observed in the visible region around 400 to 600 nm due to oxygen vacancies and interfacial Sn vacancies present in the prepared nanosamples.

**Keywords:** Chemical co-precipitation, X-ray diffraction, scanning electron microscopy, photoluminescence

### 1. Introduction

SnO<sub>2</sub> is an n-type semiconductor with wide band gap of 3.6 eV at room temperature. In nanotechnology the size of the particle plays a prominent role which influences the electrical, optical and magnetic properties. The sensitivity, selectivity and quick response of SnO<sub>2</sub> enables us to find many applications like transparent conducting electrodes, optical sensors, dye-sensitized solar cell and photocatalytic applications, chemical gas sensors [1, 5]. SnO<sub>2</sub> nanoparticles can be prepared by various synthesis routes like sol-gel, spray pyrolysis, gas-phase condensation, chemical vapour deposition, hydro-thermal, co-precipitation, laser ablation [6, 13]. Among them the simplest and cheapest wet chemical co-precipitation enables us to tune the particle size and composition of the sample. In this paper we adopted simplest and cheapest wet chemical co-precipitation method to prepare SnO<sub>2</sub> nanoparticles and studied the structural, morphological, compositional and photoluminescence properties of SnO<sub>2</sub> nanoparticles at different values of pH. Ethylene diamine tetra acetic acid was used as the capping agent for getting fine particle distribution.

### 2. Experimental and Characterization techniques

All chemicals were of analytical reagent grade and were used without further purification. SnO<sub>2</sub> nanoparticles were prepared by chemical co-precipitation method using SnCl<sub>2</sub>.2H<sub>2</sub>O as reactant material. Ethylene diamine tetra acetic acid (EDTA) was used as the capping agent. Ultrapure de-ionized water was used as the reaction medium in all the synthesis steps. In a typical synthesis, SnCl<sub>2</sub>.2H<sub>2</sub>O in 100 ml was dissolved in ultrapure de-ionized water and stirred for 30 minutes. Stirring process is carried out at a temperature of 90°C and NaOH solution was drop wisely added to the solution to adjust the pH value 7. Stirring was continued for three hours to get fine precipitation. The obtained precipitate was washed with de-ionized water for

several times. Finally, the powders were vacuum dried for 3 hours at 80°C to obtain SnO<sub>2</sub> nanoparticles. The same procedure was repeated by varying the pH = 9, 11 and 13. The dried powder was characterized for structural, morphological and optical studies.

The X-ray diffraction patterns of the samples were collected on a Rigaku D X-ray diffractometer with the Cu-K $\alpha$  radiation ( $\lambda=1.5406\text{\AA}$ ). FTIR studies were carried out by fourier transform infrared spectrophotometer (FTIR-4700typeA). Morphology and elemental composition of the prepared samples were analyzed through EDAX using Oxford Inca Penta FeTX3 EDS instrument attached to Carl Zeiss EVO MA 15 scanning electron microscope. Photoluminescence spectra were recorded in the wavelength range of 400–600 nm using PTI (Photon Technology International) Fluorimeter with a Xe-arc lamp of power 60 W and an excitation wavelength of 320 nm was used.

### 3. Results and Discussion

#### 3.1 Structural analysis

The XRD patterns for the prepared SnO<sub>2</sub> nanoparticles at different pH values are shown in Fig.1. From the fig. 1 it is obvious that the peaks are indexed as (110), (101), (200), (211), (220), (002) and (310), planes at  $2\theta$  values 26.91°, 34.11°, 38.31°, 52.17°, 54.96°, 58.22° and 62.24° that correspond to tetragonal rutile structure of polycrystalline SnO<sub>2</sub> which are in consistent with the JCPDS (No. 72-1147) data.

The average particle size was estimated Using the Debye–Scherrer's formula,

$$D = \frac{0.94\lambda}{\beta_{hkl} \cos \theta}$$

Where, D is the average Particle size,  
 $\beta_{hkl}$  is full width at half maximum of XRD peak expressed in radians and ' $\theta$ ' is the position of the diffraction peak.

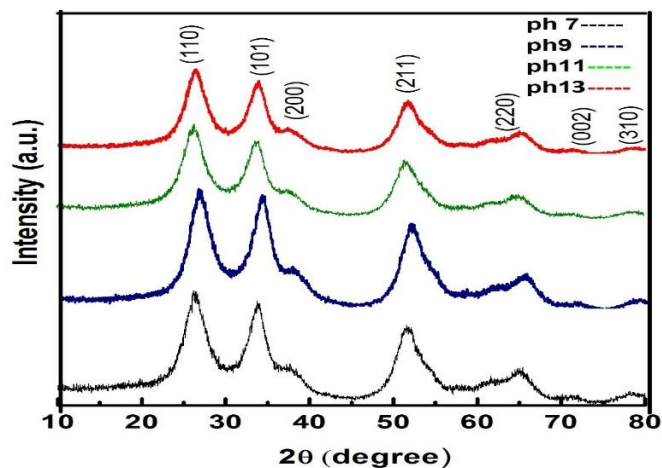


**Fig 1:** XRD patterns of SnO<sub>2</sub> nanoparticles synthesized at different pH conditions (pH - 7, 9, 11, 13)

The average crystallite sizes of as deposited SnO<sub>2</sub> nanoparticles prepared at different pH values (7, 9, 11 and 13) were of 3.2, 2.9, 3.4 and 3.5 nm, respectively. The decrease in average particle size is due to the increase in the nucleation rate with increasing the pH of the reaction mixture. The increase of particles size at higher pH is due to agglomeration of Sn-Sn atoms.

### 3.2 Morphological studies

Figure 2 shows the surface morphology of SnO<sub>2</sub> nanoparticles. Figures 2(a), 2(b), 2(c) and 2(d) show the SEM images of SnO<sub>2</sub> nanoparticles at pH= 7, 9, 11 and 13 respectively. From SEM images it was clearly observed that the particles were agglomerated. The sample prepared at pH=9 exhibits slightly decreased agglomeration compared to other samples.

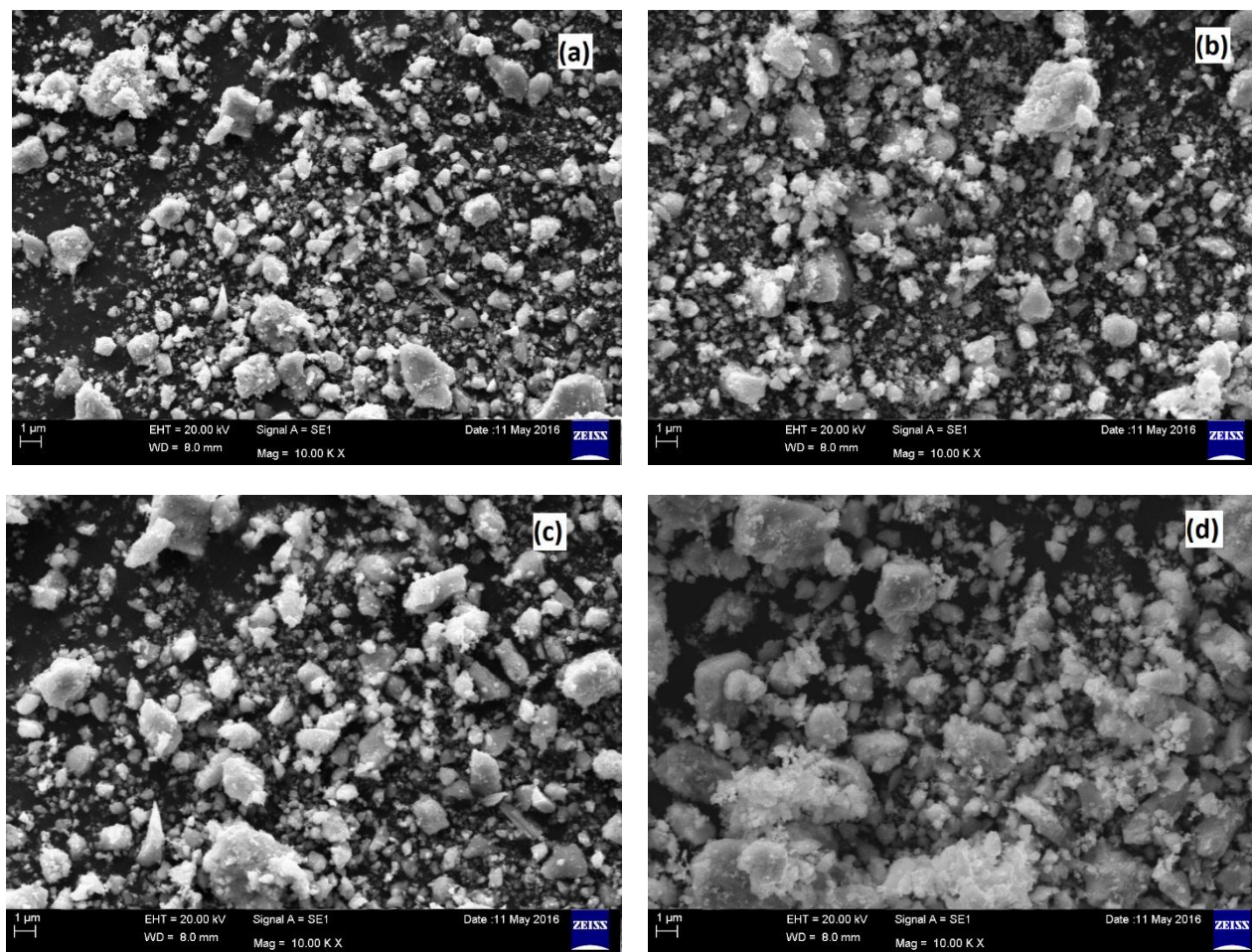


**Fig 2:** SEM images of SnO<sub>2</sub> nanoparticles prepared at (a) pH=7, (b) pH=9, (c) pH=11 and (d) pH=13

### 3.3 Compositional analysis

The EDAX profile of SnO<sub>2</sub> nanoparticles at pH= 7, 9, 11 and 13 is shown in Fig.3. It is evident from the EDAX Spectra

that no other elemental peaks other than Sn and O are observed. This confirms the effective formation of SnO<sub>2</sub> nanoparticles.

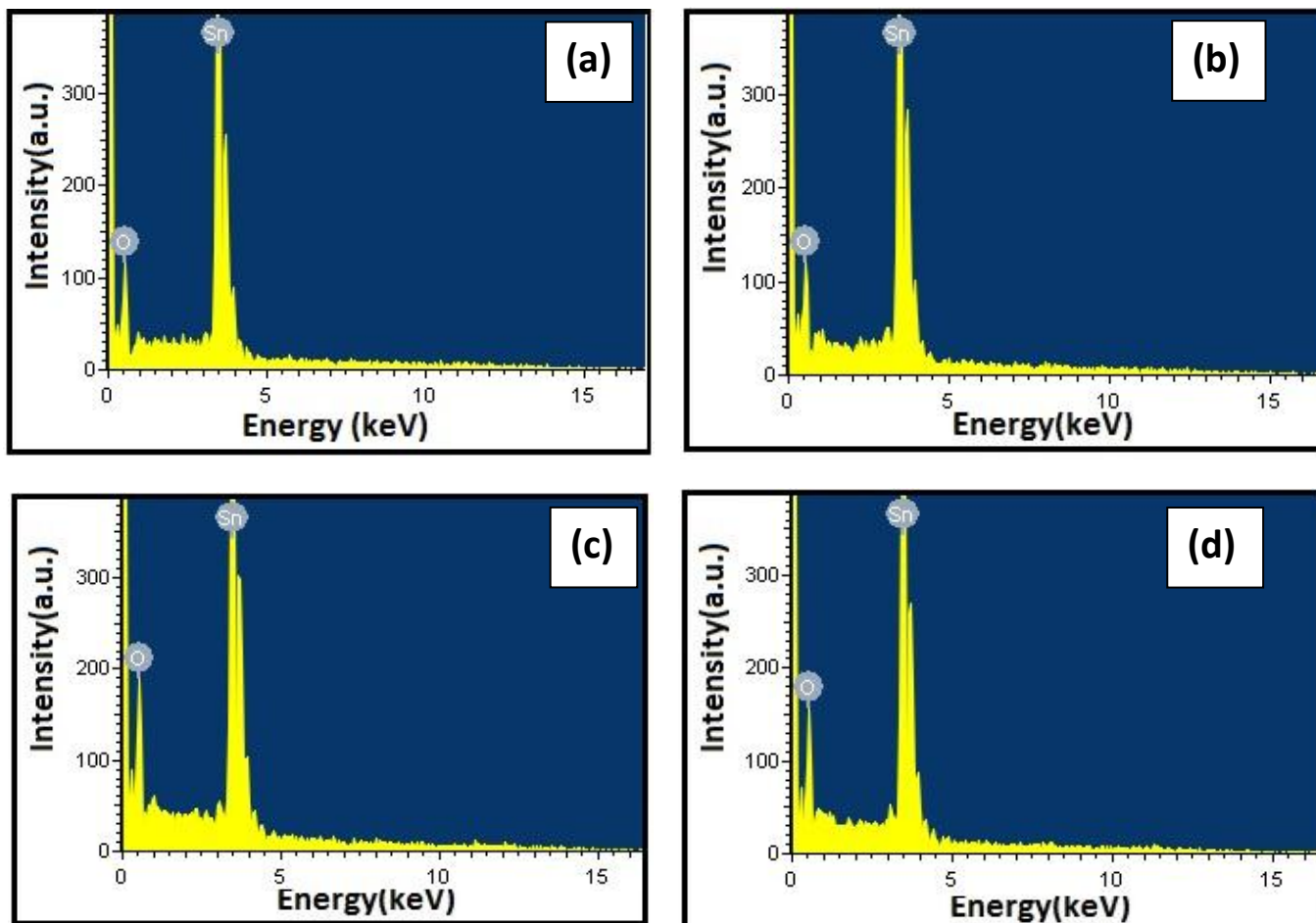


Fig 3: The EDAX profile of SnO<sub>2</sub> nanoparticles prepared at (a) pH= 7, (b) pH=9, (c) pH=11 and (d) pH= 13

### 3.4 Photo Luminescence

Fig. 4 shows the PL spectra of SnO<sub>2</sub> nanoparticles excited at 230 nm. As seen in Fig.4, all the samples showed multiple PL emission bands at 3.31 eV (375 nm), 3.16 eV (392 nm), 2.83 eV (438 nm), 2.72 eV (456 nm), 2.23 eV (557 nm), 2.07 eV (598 nm) resulting from the surface oxygen vacancies of SnO<sub>2</sub> nano samples [14, 16] no impurity peaks were observed.

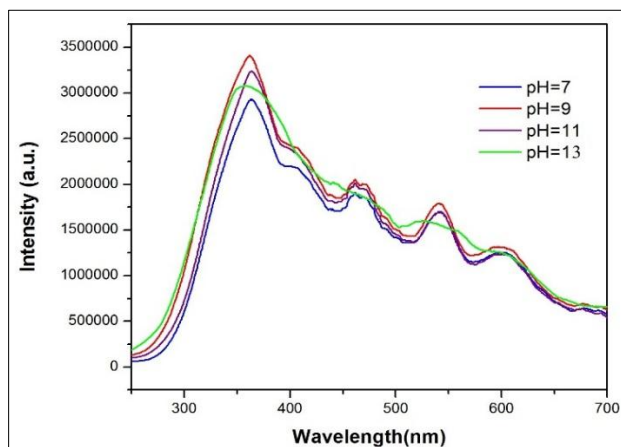
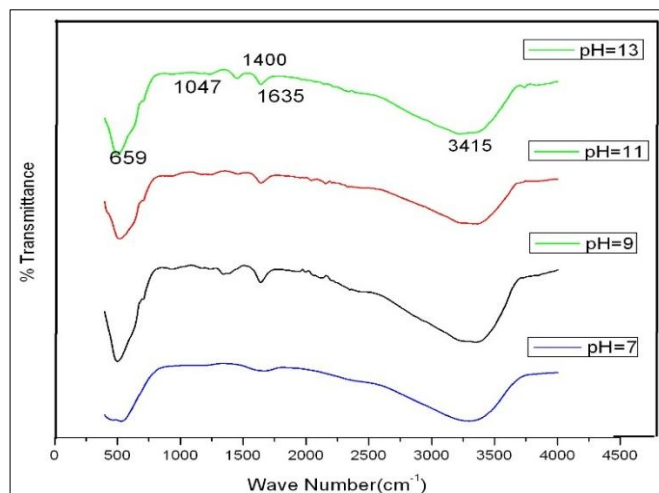


Fig 4: PL spectra of SnO<sub>2</sub> nanoparticles at pH= 7, 9, 11 and 13

It is found that the PL intensity is enhanced at pH value 9 and decreased for higher pH values. This may be due to the increment in the agglomeration and hence particle size. The emission peaks observed in the UV and Visible regions are attributed to a recombination of free excitons and defect energy levels originated due to oxygen vacancies present in the band gap of the SnO<sub>2</sub> nano particles. These oxygen vacancies are present in three different charge states  $v_o^0$ ,  $v_o^+$  and  $v_o^{2+}$  and acts as radiative centers [15].

### 3.5 FTIR studies

FTIR spectra of prepared nanosamples at different pH values are shown in fig.5. The FTIR band observed around 659 cm<sup>-1</sup> may be assign to the antisymmetric Sn-O-Sn stretching mode [17, 18]. The Sn-O-Sn band indicates the excited states of O<sup>2-</sup> in the SnO<sub>2</sub> host material. The bands 1047 and 1400 cm<sup>-1</sup> may be attributed to the bending of vibration of NO<sub>3</sub><sup>-</sup> ions present in the sample. The FTIR band observed at 1635 cm<sup>-1</sup> can be attributed to the overtones of Sn-O-Sn mode and the band at 3415 cm<sup>-1</sup> indicates the presence of O-H oscillators [19, 21].



**Fig 5:** FTIR spectra of SnO<sub>2</sub> nanoparticles prepared at pH= 7, 9, 11 and 13

#### 4. Conclusions

EDTA capped SnO<sub>2</sub> nanoparticles were successfully prepared by chemical co-precipitation method at pH values 7, 9, 11 and 13. XRD and FTIR studies revealed the tetragonal rutile structure of polycrystalline SnO<sub>2</sub> nanoparticles. From SEM micrographs, it is observed that the sample prepared at pH value 9 shows decreased agglomeration compared to other samples and EDS studies confirms the effective composition of the samples. Compared to other samples, SnO<sub>2</sub> nanoparticles prepared at Ph =9 exhibited better luminescence properties.

#### 5. References

- Hao C, Li J, Zhang Z, Ji Y, Zhan H, Xiao F, *et al.* Enhancement of photocatalytic properties of TiO<sub>2</sub> nanoparticles doped with CeO<sub>2</sub> and supported on SiO<sub>2</sub> for phenol degradation, *Applied Surface Science*. 2015; 331:17-26.
- Scott RWJ, Yang SM, Chabanis G, Coombs N, Williams DE, Ozin GA. Tin Dioxide Opals and Inverted Opals: Near-Ideal Microstructures for Gas Sensors, *Advanced Materials*. 2001; 13:1468-1472.
- Bahrami B, Khodadadi A, Kazemini M, Mortazavi Y. Enhanced CO sensitivity and selectivity of gold nanoparticles-doped SnO<sub>2</sub> sensor in presence of propane and methane Sensors and Actuators B. 2008; 133:352-356.
- Murugadoss G, Jayavel R, Kumar MR. Systematic investigation of structural and morphological studies on doped TiO<sub>2</sub> nanoparticles for solar cell applications, *Superlattices and Microstructures*. 2014; 76:349-361.
- Parthibavarman M, Renganathan B, Sastikumar D. Development of high sensitivity ethanol gas sensor based on Co-doped SnO<sub>2</sub> nanoparticles by microwave irradiation technique, *Current Applied Physics*. 2013; 13:1537-1544.
- Renard L, Babot O, Saadaoui H, Füess H, Brötz J, Gurlo A, *et al.* Nanoscaled tin dioxide films processed from organotin-based hybrid materials: an organometallic route toward metal oxide gas sensors, *Nanoscale*. 2012; 4:6806-6813.
- Chiu HC, Yeh CS. Hydrothermal synthesis of SnO<sub>2</sub> nanoparticles and their gas-sensing of alcohol, *Journal of Physical Chemistry C*. 2007; 111:7256-7259.
- Yang H, Song X, Zhang X, Ao W, Qiu G. Synthesis of vanadium-doped SnO<sub>2</sub> nanoparticles by chemical co-precipitation method, *Materials Letters*. 2003; 57:3124-3127.
- Jiang X, Wang Y, Herricks T, Xia Y. Ethylene glycol-mediated synthesis of metal oxide nanowires, *Journal of Materials Chemistry*. 2004; 14:695-703.
- Sasikala R, Shirole A, Sudarsan V, Sakuntala T, Sudakar C, Naik R, *et al.* Highly dispersed phase of SnO<sub>2</sub> on TiO<sub>2</sub> nanoparticles synthesized by polyol-mediated route: photocatalytic activity for hydrogen generation, *International Journal of Hydrogen Energy*. 2009; 34:3621-3630.
- Ren J, Yang J, Abouimrane A, Wang D, Amine K. SnO<sub>2</sub> nanocrystals deposited on multiwalled carbon nanotubes with superior stability as anode material for Li-ion batteries, *Journal of Power Sources*. 2011; 196:8701-8705.
- Harish GS, Sreedhara Reddy P, Synthesis and characterization of Ce, Cu co-doped ZnS nanoparticles, *Physica B*. 2015; 473:48-53.
- Yang H, Song X, Zhang X, Ao W, Qui G. Synthesis and characterization of SnO<sub>2</sub> nanoparticles for carbon absorbing applications, *Materials Letters*. 2003; 57:3124-3127.
- Mishra RK, Kushwaha A, Sahay PP. Influence of Cu doping on the structural, photoluminescence and formaldehyde sensing properties of SnO<sub>2</sub> nanoparticles, *RSC Advances*, 2014; 4:3904-3912.
- Sahay PP, Mishra RK, Pandey SN, Jha S, Shamsuddin M, Structural, dielectric and photoluminescence properties of co-precipitated Zn-doped SnO<sub>2</sub> nanoparticles, *Current applied Physics*. 2013; 13:479-486.
- Ahmed AS, Muhamed SM, Singla ML, Tabassum S, Naqvi AH, Azam A. Band gap narrowing and fluorescence properties of nickel doped SnO<sub>2</sub> nanoparticles, *Journal of Luminescence*. 2011; 131(1):1-6.
- Du F, Guo Z, Li G. Hydrothermal synthesis of SnO<sub>2</sub> hollow microspheres, *Materials Letters*. 2005; 59:2563-2565.
- Periathai RS, Pandiarajan J, Jaykumaran N, Prithvikumaran N. Role of temperature on the properties of SnO<sub>2</sub> Nanoparticles synthesised by Sol-Gel Process, *International Journal of Chemtech research*. 2014; 6:2132-2134.
- Das S, Kar S, Chaudhuri S. Optical properties of SnO<sub>2</sub> nanoparticles and nanorods synthesized by solvothermal process, *Journal of Applied Physics*. 2006; 99:114303(1-7).
- Abello L, Bochu B, Gaskov A, Koudryavtseva S, Lucazeau G, Roumyantseva M. Structural Characterization of Nanocrystalline SnO<sub>2</sub> by X-Ray and Raman Spectroscopy, *Journal of Solid state Chemistry*. 1998; 135:78-85.
- Gamard A, Babot O, Jousseaucne B, Rasclé MC, Toupance T, Campet G. Conductive F-doped Tin Dioxide Sol-gel Materials From Fluorinated b-Diketonate Tin(IV) Complexes. Characterization and Thermolytic Behavior, *Chemistry of Materials*. 2000; 12:3419-3426.